The Sodium-Dependent Phosphate Transporter: To Reveal Insight into Human Solute Carrier SLC20

Dysfunctions of human phosphate transporters cause numerous diseases, but the molecular mechanism of these transporters remains elusive. The structure and function of the phosphate transporter from bacterium Thermotoga maritima in a complex with phosphate and sodium provide a framework to understand PiT dysfunction and for future structure-based drug design.

Maintaining Pi balance is essential for the growth and development of all organisms; membrane-bound phosphate transporters are key factors in sustaining Pi homeostasis in humans, plants, fungi and bacteria. In humans, Pi is translocated into cells with two major secondary active transporters, *i.e.*, sodium-dependent phosphate transporter SLC20 (PiT) and SLC34 (NaPi-II) families, which prefer monovalent ($H_2PO_4^-$) and divalent (HPO_4^{2-}) phosphates, respectively.[1] A dysfunction of human phosphate transporters causes numerous diseases, including hyperphosphatemia, vascular and brain calcification and neuropsychiatric disorders, but the molecular mechanism of these transporters remains elusive. *h*PiT (*h*PiT1 and *h*PiT2) have been identified in various organs, including kidney, liver and brain. Specifically, the functional loss of *h*PiT2 in the brain can result in Pi accumulation, causing calcium phosphate deposition.

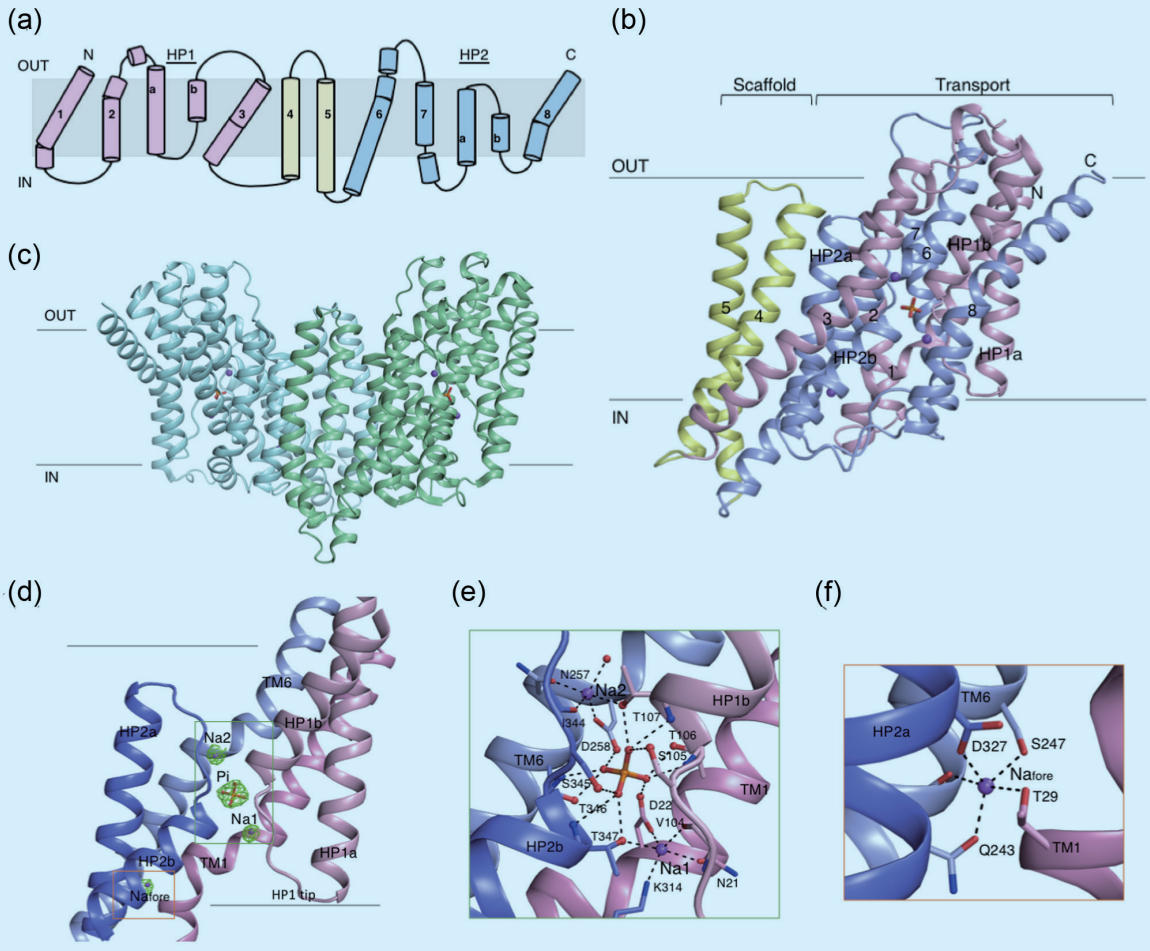

Fig. 1: (a) Topology of *Tm*PiT with 12 transmembrane helices that are divided into a transport domain with two inverted-topology repeats, N-PD001131 (TM1-3 and HP1a/b, in magenta) and C-PD001131 (TM6-8 and HP2a/b, in blue), and a scaffold domain (TM4/5, in yellow). (b) Ribbon diagram of the *Tm*PiT-Pi/Na complex consisting of a transport domain with N-PD001131 and C-PD001131 and a scaffold domain (in yellow). The Pi and Na ions are shown in CPK and as purple spheres, respectively. The transmembrane helices in (b) are coloured and numbered based on (a). (c) Ribbon diagram of the *Tm*PiT dimer. (d) F_o–F_c electron-density maps of Pi and Na are shown at 8σ and at 6σ, respectively. Transmembrane helices TM1, TM6, HP1a-HP1b and HP2a-HP2b (labeled) are involved in Pi and Na binding. The Pi- and Na-binding residues are shown in CPK and as purple spheres, respectively. (e) Magnified view of Pi-2Na binding pocket, showing interacting residues. (f) Magnified view of Na_{fore} binding, showing the penta-coordination residues. [Reproduced from Ref. 2]

The PiT contains a unique internal highly conserved domain named PD001131 present at the N- and C-termini. Within this domain are four highly conserved sequences: ΦNDΦ, GxxxxGxxVxxT, PΦSxT and IxxxWΦ (x: any amino acid; Φ: hydrophobic residue). *Thermotoga maritima* is a hyperthermophilic bacterium that makes it an ideal model organism for an integration of biochemical and structural experimental approaches. The authors show that *Tm*PiT belongs to the SLC20 family; its transmembrane domain exhibits protein characteristics and sequence homology similar to that of *h*PiT (similarity/identity 62%/38% for *h*PiT1 and 61%/39% for *h*PiT2).

To investigate the structural information for a sodium-dependent phosphate transporter, a research team led by Yuh-Ju Sun (National Tsing Hua University) solved the crystal structure of *Tm*PiT, a homology of *h*PiT. They measured the phosphate-binding affinity as 57.0 ± 1.1 μM and determined the uptake ability of *Tm*PiT being driven by sodium. The crystal structure of *Tm*PiT bound to sodium and phosphate (*Tm*PiT-Na/Pi) is in an inward occluded state and exits as a dimer, with the two subunits showing distinct conformations. All diffraction data sets were collected at **TPS 05A** in NSRRC.[2]

The *Tm*PiT-Pi/Na complex is shown in **Figs. 1(a) and 1(b)**; the transport and scaffold domains are formed with 12 transmembrane helices. The transport domain of *Tm*PiT assumes a "5+5" fold and is arranged into two inverted repeats annotated as PD001131, N-PD001131 (TM1/TM2/HP1a-HP1b/TM3) and C-PD001131 (TM6/TM7/HP2a-HP2b/TM8). HP1a-HP1b (HP1) and HP2a-HP2b (HP2) are re-entrant helical hairpins that have been reported in the transporters of elevator type, such as aspartate transporter Gltph and dicarboxylate transporter VcINDY. *Tm*PiT is a dimer with dimensions 83 Å × 61 Å × 55 Å; the N- and C-termini are located in the extracellular region (**Fig. 1(c)**). The dimer interface between two subunits (A and B) is formed with TM2/7 from the transport domain and TM4/5 from the scaffold domain and has a buried area 1283.7 Å^2.

In the *Tm*PiT-Pi/Na complex structure, three sodium ions were found (**Fig. 1(d)**): two sodium ions and one phosphate (hereafter Pi-2Na) were located at the core of *Tm*PiT; the third sodium (Na_{fore}) was situated near the inner membrane boundary. The Pi-2Na binding site is formed with TM1, loop HP1a-HP1b l(HP1 tip), TM6 and loop HP2a-HP2b (HP2 tip) (**Figs. 1(d) and 1(e)**). The phosphate is associated with two sodium ions as "Na1-Pi-Na2" through two aspartates, D22 and D258. A phosphate was located 4.8 Å from each sodium ion. This phosphate was tightly bound *via* 12 interactions with eight conserved residues, including D22 (TM1), D258 (TM6) and six polar residues, S105/T106/T107 (HP1b) and S345/T346/T347 (HP2b) (**Fig. 1(e)**). Both Na1 and Na2 are bound within a penta-coordinated interaction with conserved residues Asp/Asn/Thr. All these Pi-2Na-binding residues are highly conserved in PiT families; D22 and D258 are involved in both Pi and Na binding. In addition to Pi-2Na binding, a third sodium, Na_{fore}, was identified near TM1, TM6 and HP2a with penta-coordination through residues T29, Q243, S247 and D327 (**Fig. 1(f)**), which are highly or partially conserved in the PiT.

In the *Tm*PiT-Pi/Na complex, there are significant structural differences between subunits A and B, which are reflected in a root-mean-square deviation 1.8 Å for the Cα atoms mainly in TM8 and intracellular loops L7 and LHP2. The accessible volumes of this region, calculated using CASTp, are 68 Å^3 and 252 Å^3 for subunits A and B, respectively (**Figs. 2(a) and 2(b)**). Conformational changes in the *Tm*PiT-Pi/Na complex in loops L7, LHP2 and TM8 between subunits A and B indicate that the subunits might have distinct functional states. They might control the inner gate during phosphate and sodium release on assuming closed and open states in subunits A and B, respectively.

Interestingly, particular structural characteristics of *Tm*PiT reflect those reported in disease-associated mutations in *h*PiT. Several mutations in *h*PiT2 have been associated with neuropsychiatric disorders and primary familial brain calcification.[3] To understand how these mutations might affect *h*PiT function, the authors mapped these *h*PiT mutations onto the *Tm*PiT-Pi/Na complex structure (**Fig. 3**); they found a significant correlation between their *Tm*PiT results and

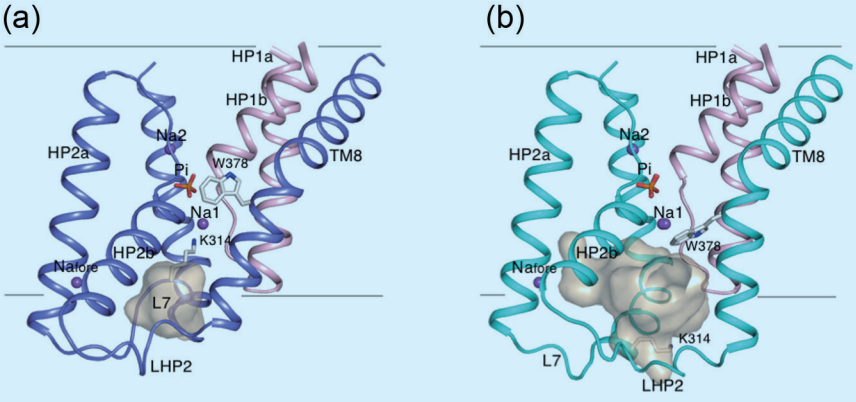

Fig. 2: The structures of subunits A and B around inner gates are shown in (a) and (b), respectively. Two inverted, repeated domains are shown: HP1 from N-PD001131 (in magenta in both subunits) and HP2 and TM8 from C-PD001131 (in blue and cyan for subunits A and B, respectively). The structures shown include Pi and Na, and residues K314 and W378. The Pi and Na ions are shown in CPK and as purple spheres, respectively. Residues K314 and W378 are shown in CPK. The accessible volumes of the exit region were calculated with CASTp30 and are shown in brown. [Reproduced from Ref. 2]

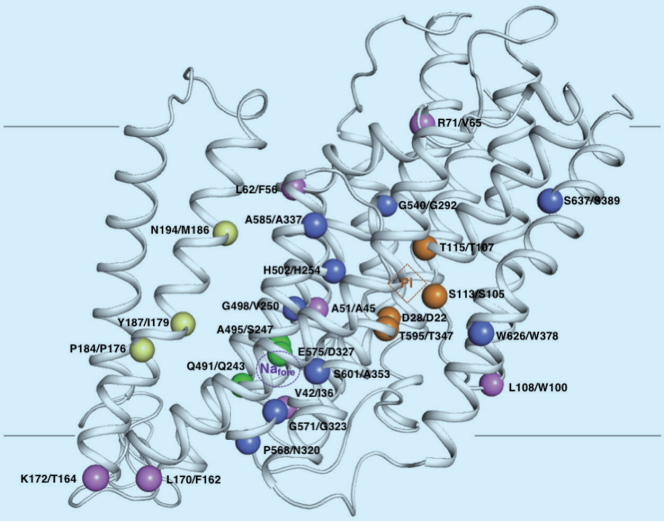

Fig. 3: Variants in *h*PiT2 linked to brain calcification disease were mapped onto the modeled *h*PiT2 structure. Variants are shown as spheres and grouped into five categories: Pi-binding (orange), Na-binding (green), N-PD001131 (pink), C-PD001131 (blue) and dimer (yellow). The Hs/Tm number is also labelled. The Pi and Na binding sites are indicated with dashed outlines. [Reproduced from Ref. 2]

clinical data from variants in *h*PiT. For example, the variant residues in hPiT are all found at essential positions or are involved in sodium and phosphate binding; some are near the inner membrane and might regulate Pi transport; a few are in the dimerization domain; others are located in the extracellular soluble (S) domain. These findings highlight how the *Tm*PiT structural data might inform the molecular mechanisms underlying human diseases associated with mutations in *h*PiT.

In summary, the *Tm*PiT-Pi/Na complex contains a phosphate and three sodium ions tightly bound with TM1/6 and HP1/HP2. Structural differences occur between subunits A and B near the inner gate, in loops L7/LHP2 and TM8. These findings provide a structural basis for disease-causing mutations in *h*PiT. *Tm*PiT is the first complete structural study of a sodium-dependent phosphate transporter. The resolved three-dimensional structure of *Tm*PiT might help establish therapeutic targets for PiT dysfunction diseases. (Reported by Jia-Yin Tsai, National Tsing Hua University)

This report features the work of Yuh-Ju Sun and her collaborators published in Sci. Adv. ***6****, eabb4024 (2020).*

TPS 05A Protein Microcrystallography

- Protein Crystallography
- Biological Macromolecules, Protein Structures, Life Science

References

1. I. C. Forster, N. Hernando, J. Biber, H. Murer, Mol. Aspects Med. **34**, 386 (2013).
2. J.-Y. Tsai, C.-H. Chu, M.-G. Lin, Y.-H. Chou, R.-Y. Hung, C.-D. Hsiao, Y.-J. Sun, Sci. Adv. **6**, eabb4024 (2020).
3. R. R. Lemos, E. M. Ramos, A. Legati, G. Nicolas, E. M. Jenkinson, J. H. Livingston, Y. J. Crow, D. Campion, G. Coppola, J. R. Oliveira, Hum. Mutat. **36**, 489 (2015).